Cellular Signalling 53 (2019) 400–412

Contents lists available at ScienceDirect

Cellular Signalling

journal homepage: www.elsevier.com/locate/cellsig

Bevacizumab induces inflammation in MDA-MB-231 breast cancer cell line and in a mouse model

Layal EL-Hajjar[a,1], Nour Jalaleddine[a,1], Abdullah Shaito[b], Kazem Zibara[c], Jalal M. Kazan[d,2], Jamal El-Saghir[d], Marwan El-Sabban[d,*]

[a] Department of Biological and Environmental Sciences, Faculty of Science, Beirut Arab University, Beirut, Lebanon
[b] Department of Biological and Chemical Sciences, Faculty of Arts and Sciences, Lebanese International University, Beirut, Lebanon
[c] ER045– Laboratory of Stem Cells, PRASE, Biology Department, Faculty of Sciences, Lebanese University, Beirut, Lebanon
[d] Department of Anatomy, Cell Biology and Physiological Sciences, Faculty of Medicine, American University of Beirut, Beirut, Lebanon

ARTICLE INFO

Keywords:
Inflammation
Angiogenesis
NF-κB
Connexin 43
Breast cancer
Metastasis

ABSTRACT

Background: Bevacizumab or Avastin® (Av) is an anti-vascular endothelial growth factor agent. It does not improve survival of breast cancer patients due to development of refractoriness. Av treatment was shown to increase inflammation in a diabetic mouse model, and also to induce epithelial-to-mesenchymal transition of non-transformed breast epithelia. This study aimed to understand if the Av-induced inflammatory microenvironment could be a mechanism of Av refractoriness. Expression profiles of inflammatory mediators, *in vitro* in MDA-MB-231 cells, *in vivo* in a mouse model xenografted with MDA-MB-231 cells and from archived cases of human breast carcinoma tissues were evaluated. Gap junctions are also crucial for angiogenesis and tumor cell extravasation. The effect of connexin 43 (Cx43) overexpression on the expression of inflammatory markers in MDA-MB-231 cells treated with Av was assessed.

Methods: MDA-MB-231 cells, control or overexpressing Cx43, were used in this study. Proliferation and invasion assays were performed. Quantitative PCR, ELISA and western blotting were performed to assess the regulation of inflammatory mediators and other factors upon Av treatment. Immunofluorescence was performed to document the translocation of Nuclear Factor-kappa B p65.

Results: Breast cancer tissues had elevated transcriptional levels of inflammatory mediators. Av treatment increased expression levels of inflammatory mediators and metastatic factors *in vitro* and *in vivo*. Interestingly, overexpressing Cx43 in MDA-MB-231 cells alleviated the inflammatory effects induced by Av treatment.

Conclusion: This study attributes Av refractoriness to the Av therapy-induced inflammatory microenvironment.

1. Introduction

Triple negative breast cancer (TNBC), high-grade invasive ductal carcinoma, is characterized by the lack of estrogen receptor (ER), progesterone receptor (PR), and human epidermal growth factor receptor 2 (HER2) [1–3] rendering it refractory to targeted therapies [1,2,4–6]. TNBCs, though heterogeneous, are mostly high-grade invasive ductal carcinomas that frequently affect younger patients and follow an aggressive treatment course [1,2,4–6]. TNBC is refractory to the effective targeted therapy used in luminal and HER2-positive breast carcinomas due to the absence of ER, PR, and HER2 [3,7].

Massive data support a central role for angiogenesis in breast cancer growth and metastasis. Vascular endothelial growth factor (VEGF) is a major regulator of angiogenesis. Avastin® (Av) is an anti-VEGF agent that has been FDA approved for the treatment of various cancers including breast cancer [8,9]. Despite being an effective treatment at early stages, Av does not improve overall survival since patients develop resistance [10,11]. It is crucial to understand the mechanism of Av refractoriness to improve its clinical outcomes. Tumors bypass antiangiogenic therapies, such as Av therapy, *via* a variety of mechanisms

Abbreviations: Cx43, connexin 43; VEGF, vascular endothelial growth factor; RAGE, receptor of advanced glycation end products; IL-1β, interleukin-1β; TNF-α, tumor necrosis factor-α; NF-κB, nuclear factor-κB; MMP, matrix metalloproteinase; CD44, cluster of differentiation 44; GFP, green fluorescent protein; FFPE, formalin-fixed paraffin-embedded; IκB-α, inhibitor of kappa B; PVDF, polyvinylidene fluoride; PBS, phosphate buffered saline

* Corresponding author.
E-mail addresses: kzibara@ul.edu.lb (K. Zibara), jalal.kazan@mail.mcgill.ca (J.M. Kazan), jae13@mail.aub.edu (J. El-Saghir), me00@aub.edu.lb (M. El-Sabban).
[1] Contributed equally.
[2] Current address: Department of Biochemistry/Goodman Cancer Research Centre, McGill University, Montréal, Québec, Canada H3G 1Y6.

https://doi.org/10.1016/j.cellsig.2018.11.007
Received 27 July 2018; Received in revised form 10 November 2018; Accepted 12 November 2018
Available online 14 November 2018
0898-6568/

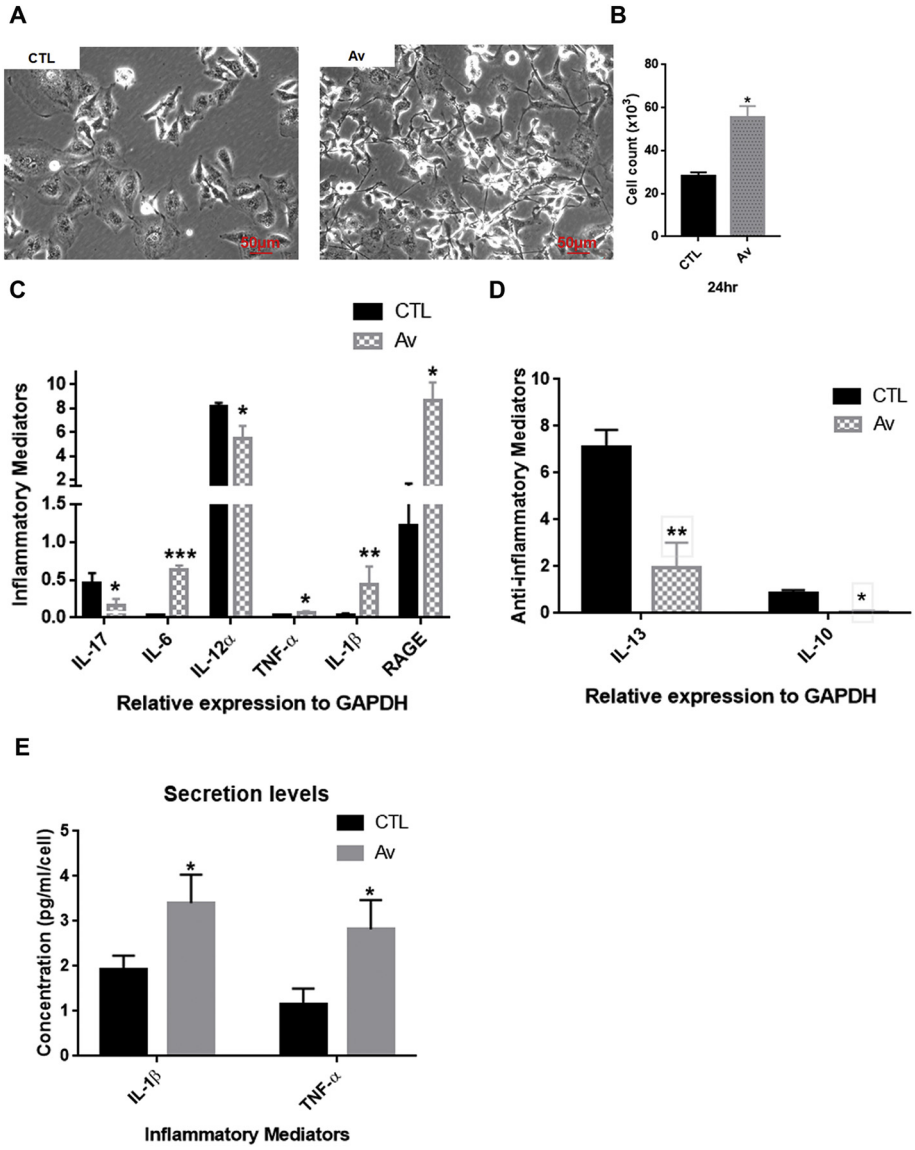

Fig. 1. Av-treated MDA-MB-231 cells acquire a more mesenchymal-like morphology (A) and increases cell proliferation (B) and mRNA expression level of inflammatory mediators. (C) qPCR showing mRNA levels of RAGE, IL-1β, TNF-α, IL-12a, IL-6 and IL-17 on Av-treated MDA-MB-231 cells, (D) IL-13 and IL-10. (E) TNF-α concentration (pg/ml/cell) in Av-treated MDA-MB-231 cells for 24 h and (E) IL-1β. Data for each target mRNA were normalized to GAPDH. Results are representative of three different independent experiments. *, **, *** indicate $P < .05$, $P < .001$, $P < .0001$, respectively.

[12]. Av induces extracellular matrix (ECM) remodeling due to induced hypoxia [13]. It also increases inflammation in diabetic mice [14]. Hypoxia and inflammation are major culprits during cancer progression and are intimately linked [15–17]. In inflammatory breast cancer (IBC), the most aggressive form of breast cancer, intermittent hypoxia activating nuclear factor kappa B (NF-κB) pathway is behind its high metastatic potential [18]. The inflammatory mediators in the tumor microenvironment promote growth and metastasis by inducing epithelial-to-mesenchymal transition (EMT) of non-transformed breast epithelial cells [19]. Cancer cells communicate with endothelial cells *via* paracrine and heterocellular communication, making both VEGF and gap junctions (GJs) crucial in extravasation and metastasis [20,21]. GJs are channels allowing the exchange of metabolites and electric signals between adjacent cells. They are made of connexin proteins which can form non-junctional hemichannels that allow the paracrine interaction with the extracellular milieu [22–24]. VEGF was found to mediate autocrine regulation of myocyte Cx43 [25]. Moreover, hypoxia dysregulates Cx43 by modulating NF-κB activity [26]. In fact, over-expression of Cx43 in breast cancer cells reversed their malignant properties and suppressed tumor growth and angiogenesis *in vivo* [27–29].

The aim of this study was to investigate the role of the inflammatory milieu in refractoriness to Av and to evaluate if Cx43 overexpression in MDA-MB-231, a highly metastatic breast cancer cell line, would attenuate the inflammatory effects of Av *in vitro* and *in vivo*.

2. Materials and methods

2.1. Cell culture

MDA-MB-231, a highly metastatic triple-negative mammary adenocarcinoma cell line, MDA-MB-231 and Cx43-Dendra (MDA-Cx43D, overexpressing Cx43) were used in this study [30].

2.2. Lentiviral transduction and cell sorting

MDA-Cx43D cells are MDA-MB-231 cells overexpressing Cx43 in fusion with Dendra, a photo-convertible fluorescent protein from green to red. To generate MDA-Cx43D cells, a *pCSCW-Cx43-Dendra2* lentiviral

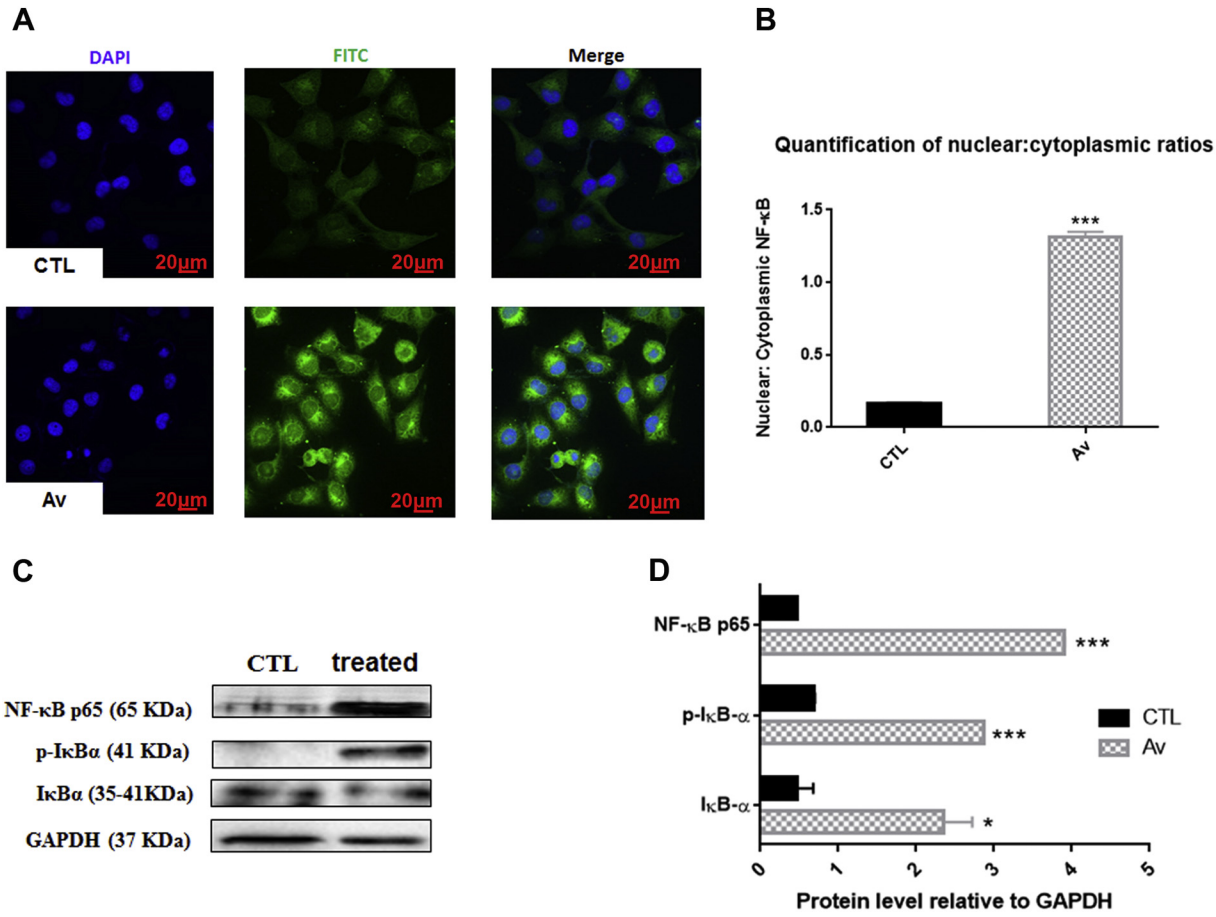

Fig. 2. Av treatment induced the activation of NF-κB pathway. (A) Immunofluorescence staining of Rel A in MDA-MB-231 cells treated with Av for 24 h. (B) Densitometry quantification of nuclear:cytoplasmic ratios of NF-κB p65 in a time course study of NF-κB nuclear translocation in MDA-MB-231 cells. (C) Western blot and (D) Densitometric analysis for NF-κB p65, p-IκBα and IκBα and GAPDH from Av-treated MDA-MB-231 cells for 24 h. Values represent the average fold change of NF-κB p65, p-IκB-α and IκB-α expression, normalized to GAPDH, and relative to control, for a total of three western blots. Results are representative of three different independent experiments. *, **, *** indicate $P < .05$, $P < .001$, $P < .0001$, respectively.

vector was co-transfected with packaging plasmids, using calcium phosphate method, into 293 T cells, for the production of viral particles. The produced viral particles were used to infect MDA-MB-231 cells. Following viral transduction, MDA-MB-231 cells were sorted to attain > 90% Dendra-fluorescence positive cells by fluorescence-assisted cell sorting (FACS Aria-SORP, Becton Dickenson, San Jose, USA). Cells were maintained in RPMI-1640 medium (Lonza, USA) supplemented with 10% fetal bovine serum (FBS) and 1% penicillin-streptomycin (Sigma, USA), and incubated at 37 °C in a humidified incubator (95% air, 5% CO_2). Cells were treated with bevacizumab (Avastin®, Genentech, USA) at 50 μg/ml for 24 h [31].

2.3. Flow cytometric analysis of CD44 expression

The expression of the cell surface glycoprotein CD44 was evaluated by flow cytometry and data were analyzed using the FlowJo software (BD Biosciences, USA). Briefly, cells were treated by Av for 24 h, harvested and labeled with APC-tagged CD44 antibody (BioLegend, USA). Finally, cells were analyzed by BD FACS Aria II SORP (BD Biosciences, USA).

2.4. Xenograft mouse model of solid cancer metastasis

This study was approved by the Institutional Animal Care and Utilization Committee of the American University of Beirut (IACUCC# 10–07-154). Mice were xenografted with MDA-MB-231 cells using our previously established protocol [32]. Briefly, immune-deficient NSG mice (NOD.Cg-*Prkdc*scid *Il2rg*tm1Wjl/SzJ, Jackson Laboratory, USA) were injected subdermally (*s.d.*) with 2×10^6 MDA-MB-231 cells. At the day of injection, mice were randomized into two experimental groups: control or Av-treated. Av (10 mg/kg) was administered intraperitoneally (*i.p.*), for 4 weeks, twice per week. Cell culture media was used as a vehicle control.

2.5. Animal tissue harvesting

At weeks 5 or 9, mice were anesthetized with isoflurane and euthanized by cervical dislocation. Lung samples were collected and snap frozen in liquid nitrogen and then stored at −80 °C for later RNA and protein extractions.

2.6. Patients and specimens

Samples of breast carcinoma patients were retrieved from the Pathology Department at the American University of Beirut Medical Center and Hammoud Hospital University Medical Center. This study was performed according to the regulations of the IRB committee at the American University of Beirut Medical Center (reference number: PALM. FB. 01). Patients were females with no treatment history, classified into 3 groups: Group 1 (11 TNBC cases), group 2 (11 $ER^-/PR^-/HER2^+$ cases) and group 3 (15 $ER^+/PR^+/HER2^-$ cases).

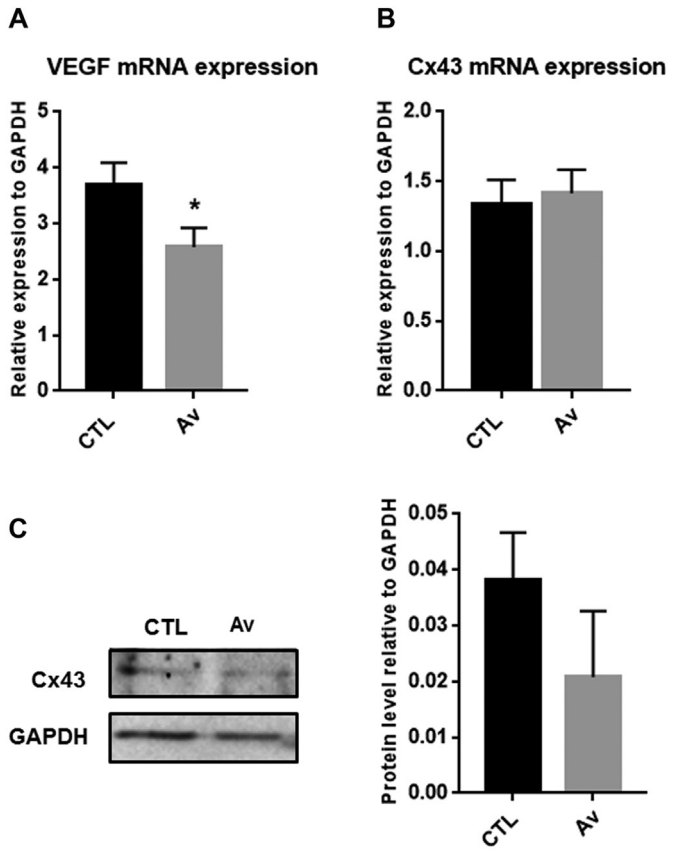

Fig. 3. Av treatment decreases transcriptional expression of VEGF. (A and B) qPCR showing mRNA levels of Cx43 and VEGF in 24 h Av-treated MDA-MB-231 cells. Data of each target mRNA were normalized to GAPDH. (C) Western blot analysis of Cx43 and GAPDH in Av-treated MDA-MB-231. Densitometry quantification of Cx43 and GAPDH bands were done using Image Lab software. Values represent the average fold change in Cx43 expression, normalized to GAPDH, and relative to control non-transduced cells, for a total of three western blots. Results are representative of three different independent experiments. *, **, *** indicate $P < .05$, $P < .001$, $P < .0001$, respectively.

2.7. RNA extraction and quantitative PCR (qPCR)

Total RNA was isolated from cells or mouse tissues using Nucleospin RNA II Kit (Machery-Nagel, USA) or Trizol reagent (Life Technologies, USA), respectively. Total RNA from formalin-fixed paraffin-embedded (FFPE) breast specimens was extracted using the RecoverALL Total Nucleic Acid Isolation Kit (Ambion, USA). 1 μg of total RNA was first reverse-transcribed to cDNA using RevertAid 1st strand cDNA synthesis kit (Thermo, USA) and then amplified by qPCR using iQ SYBR Green Supermix in a CFX96 system (Bio-Rad Laboratories, USA). Human primers are listed in Supplementary Table 1. ΔΔCq was used to calculate the relative fold change in gene expression after normalization to the housekeeping gene, GAPDH.

2.8. Analysis of protein expression by western blot

Following cell lysis, proteins were resolved using SDS–PAGE, transferred overnight to PVDF membranes (Bio-Rad Laboratories, USA), then incubated with primary and secondary antibodies. Primary antibodies for VEGF, NF-κB p65, NF-κB p50, IκB-α, p-IκB-α (Santa Cruz Biotechnology, Santa Cruz, CA), Cx43 (Invitrogen, USA), IL-1β, TNF-α, and GAPDH (Abcam, USA) were used. Protein bands were visualized by chemiluminescence and quantified by densitometry using Image Lab Software (Bio-Rad Laboratories, USA).

2.9. Enzyme-linked immunosorbent assay

The levels of IL-1β, TNF-α, and VEGF secreted from cells treated or not with Av were measured using specific ELISA kits (BD Biosciences, USA).

2.10. Immunofluorescence

MDA-MB-231 and MDA-Cx43D treated or not with Av were fixed, permeabilized and incubated with NF-κB p65, IκB-α or p-IκB-α primary antibodies followed by secondary antibodies. Nuclei were counterstained with Hoechst 33342 (Eugene, USA) and samples were imaged using a laser scanning confocal microscope (LSM 710, Carl Zeiss, Germany).

2.11. Immunofluorescence staining of paraffin-embedded tissues

Lung tissue sections were obtained from control or Av-treated mice. Tissues, 5-μm thick, were immunostained for IκB-α and p-IκB-α expression. Sections were heated to 50 °C for 40 min, deparaffinized in xylol, and then rehydrated. Following antigen retrieval sections were washed with deionized water and blocked with 5% normal goat serum in PBS for 1 h in a humidified chamber. Sections were incubated with primary antibodies overnight at 4 °C, followed by washing and incubation with IgG-conjugated secondary antibody (Alexa 488 and Texas Red). The sections were then washed with PBS, mounted with Prolong Anti-fade, and observed under the fluorescent microscope (LSM 710, Carl Zeiss, Germany).

2.12. Gelatin zymography

Proteins extracted from control or Av-treated cells were resolved on SDS-PAGE gel containing gelatin as a substrate. Gels were incubated in substrate buffer overnight at 37 °C. Gels were then stained with Coomassie blue (R250) and visualized using Chemidoc MP Imaging System. Band intensity was analyzed using Image Lab Software (Bio-Rad Laboratories, USA).

2.13. Real-time migration, invasion and proliferation assay

Quantitative analysis of the effect of Av treatment on the migration, invasion and proliferation of MDA-MB-231 and MDA-Cx43D was performed with slight modifications using xCELLigence Real-time Cell Analyzer (RTCA, Roche Applied Science, USA) [33]. Control or Av-treated cells were re-suspended in serum-free media and seeded in the upper chamber of the RTCA CIM-plates, coated with Matrigel for invasion assays or left uncoated for the migration assays. For proliferation assays, cells were seeded in *E*-plates. Migration, invasion and proliferation were monitored every 15 mins for a minimum of 18 h, by recording cell impedance produced as the cells attached and detached from the gold electrodes in the CIM and E-plates. The generated cell index (CI) correlates directly with cell number. Data were expressed as bar graphs of CI % of control.

2.14. Statistical analysis

Results are expressed as individual data or as the average ± SEM. Statistical comparisons were performed using Student's *t*-test or ANOVA in order to determine statistical significance. *P* value was determined and significance level was set at $P < .05$. Microsoft Excel and GraphPad Prism 7 were used to perform statistical analysis.

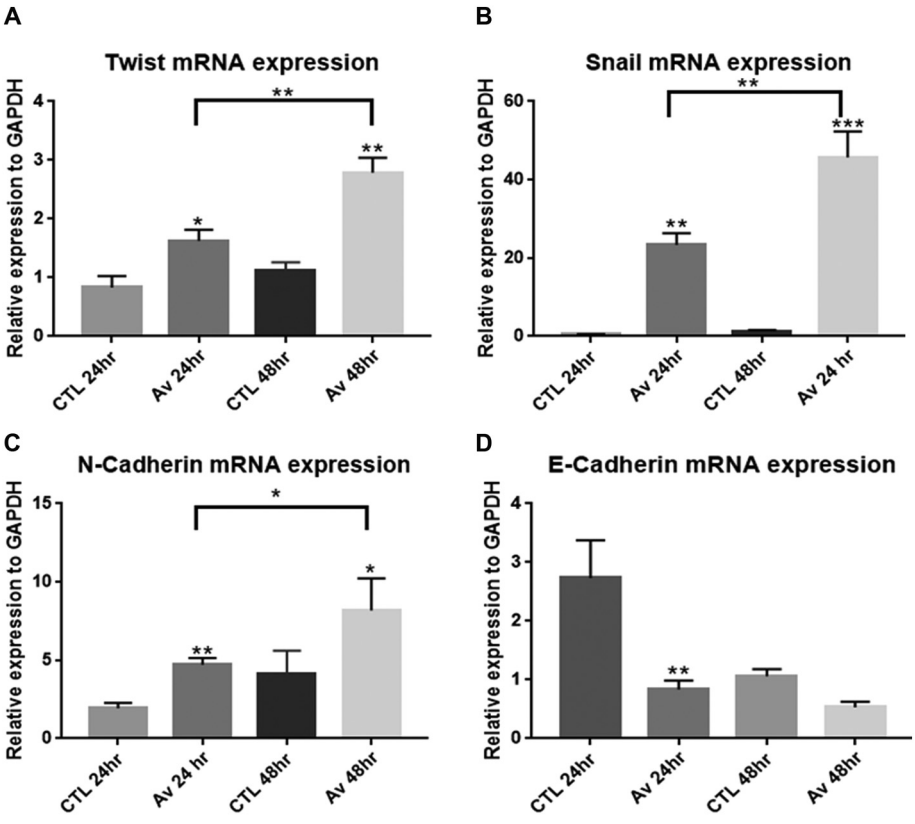

Fig. 4. Av treatment increases mRNA levels of EMT markers and decreases mRNA levels of MET marker, *E*-Cadherin. (A) qPCR showing the effect of Av treatment of MDA-MB-231 cells on Twist mRNA expression (B) Snail (C) N-Cadherin and (D) E-Cadherin. Data foreach target mRNA were normalized to GAPDH. Results are representative of three different independent experiments. *, **, *** indicate $P < .05$, $P < .001$, $P < .0001$, respectively.

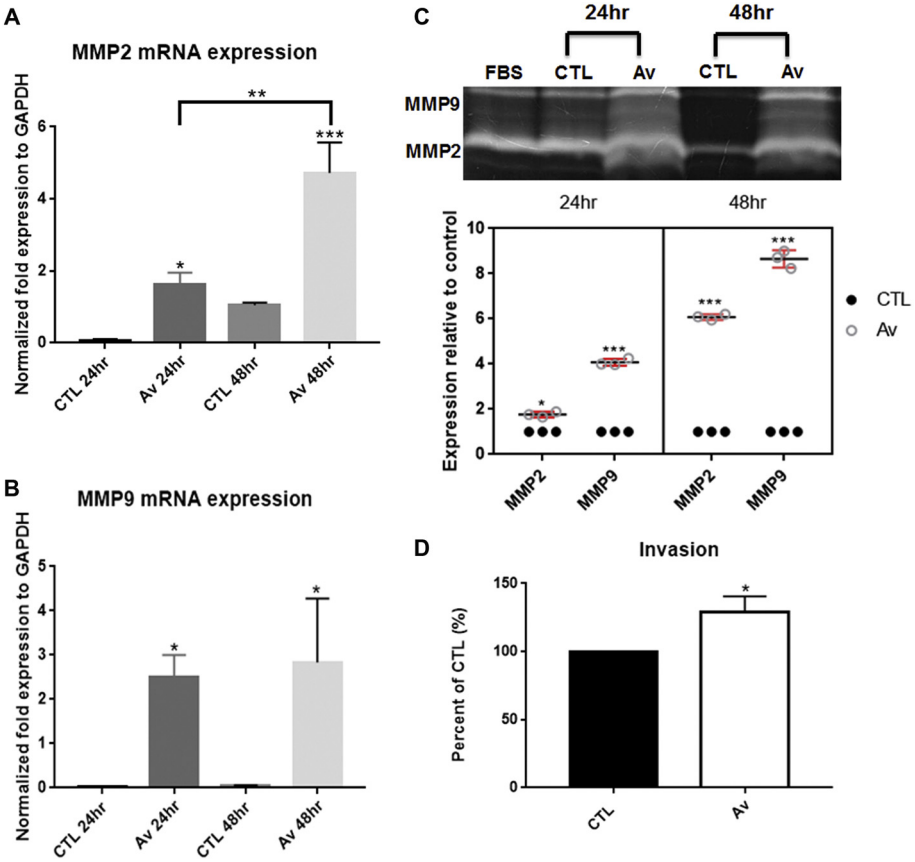

Fig. 5. Av treatment increases mRNA levels and activity of MMP2 and MMP9. qPCR showing the effect of Av treatment in MDA-MB-231 cells on transcriptional levels of MMP2 (A) and MMP9 (B). Data for each target mRNA were normalized to GAPDH. (C) Gelatin zymography of Av-treated MDA-MB-231 cells. FBS was used as an internal control. Proteins were separated on a gel containing gelatin, the substrate of MMPs, in order to assess the activation status and levels of these enzymes. Densitometry quantification of MMP2 and MMP9 bands was then performed using Image Lab software. Quantification of each band was normalized to control. (D) Invasion of MDA-MB-231 cells. Quantification graphs normalized cell index values, relative to controls, for 24 h pre-treatment. Cell impedance readings were taken every 15 min for a minimum of 18 h. Results are representatives of two independent experiments ($n = 2$). Results are representative of three different independent experiments. *, **, *** indicate $P < .05$, $P < .001$, $P < .0001$, respectively.

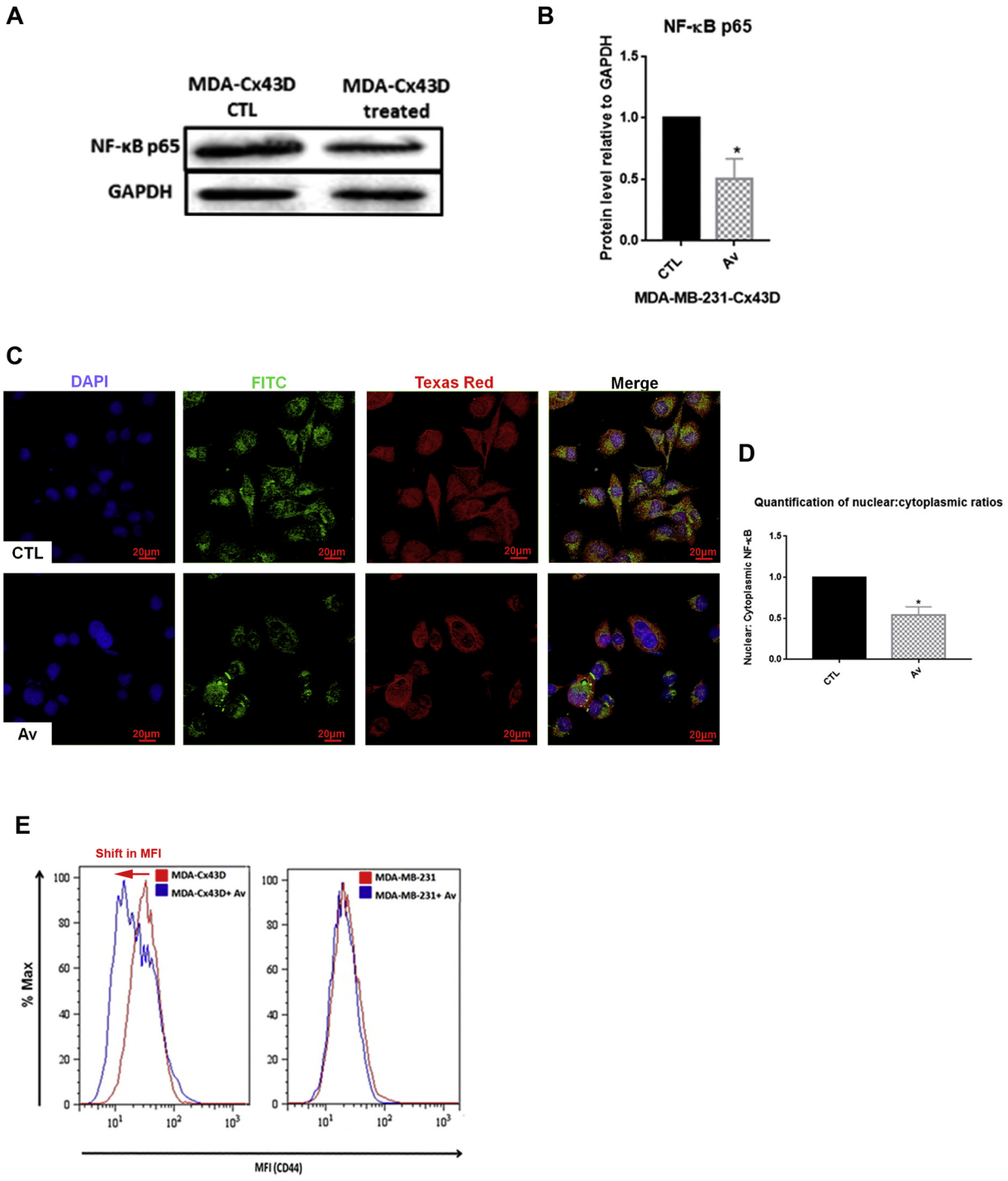

Fig. 6. Overexpression of Cx43 enhances sensitivity of MDA-MB-231 cells to Av treatment. (A) Western blot analysis of total protein obtained from cell lysates of Av-treated MDA-Cx43D cells for NF-κB p65 and GAPDH. (B) Densitometric quantification of NF-κB p65. (C&D) Immunofluorescence staining of RelA in MDA-Cx43D cells treated with Av for 24 h followed by quantification of nuclear:cytoplasmic ratios of Rel A in a time course study of NF-κB nuclear translocation. (E) A representative flow cytometry graph where the shift in MFI is shown. Results are representative of three different independent experiments. *, **, *** indicate $P < .05$, $P < .001$, $P < .0001$, respectively.

3. Results

3.1. In vitro study

3.1.1. Av treatment induces a mesenchymal like phenotype in MDA-MB-231 cells

MDA-MB-231 cells treated with Av showed a change in morphology towards a more mesenchymal-like shape compared to a more cuboidal shape in control cells (Fig. 1A). This morphological change was accompanied by a significant 50% increase in proliferation of MDA-MB-231 cells treated with Av compared to control untreated cells (Fig. 1B).

3.1.2. Av treatment increases inflammation in MDA-MB-231 cells

The expression of different pro-inflammatory mediators (IL-17, IL-6, IL-12a, IL-1β, TNF-α and RAGE) and the anti-inflammatory cytokines IL-10 and IL-13 was examined in Av-treated cells using qPCR. Results

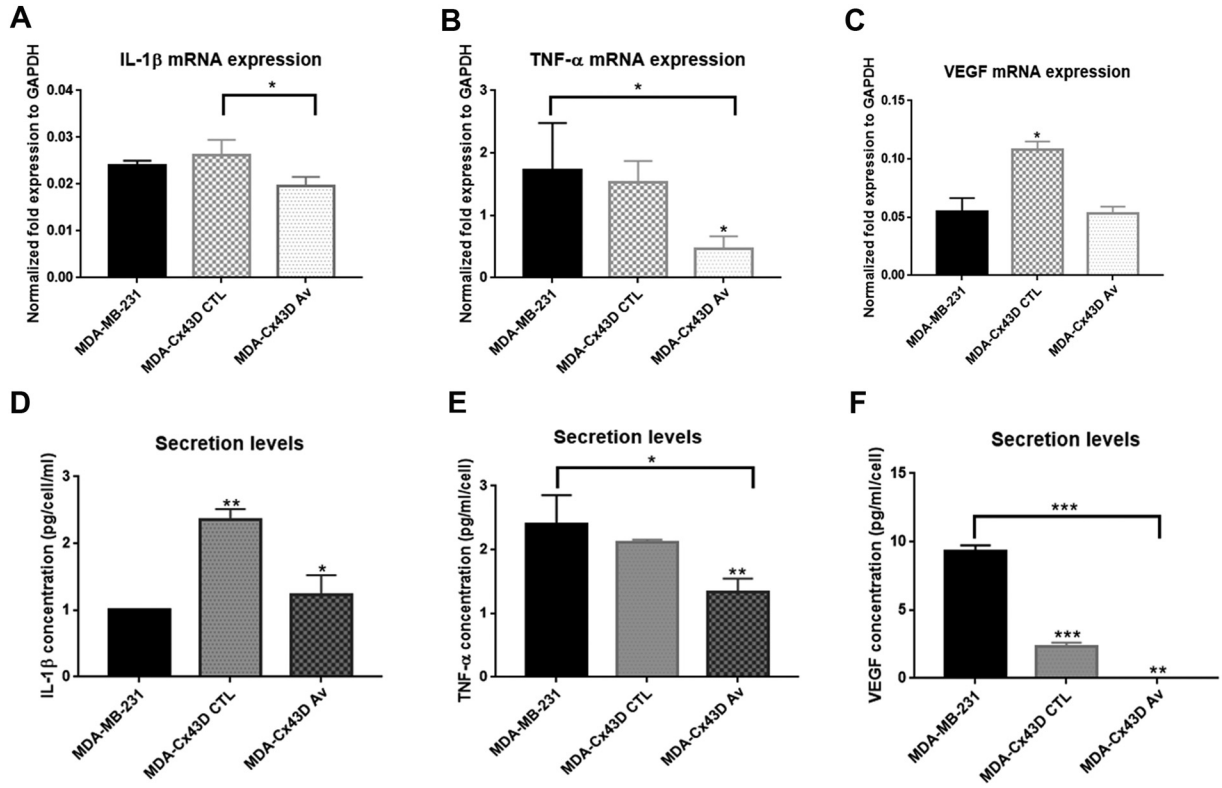

Fig. 7. Cx43 overexpression leads to the downregulation of the mRNA and protein levels of inflammatory mediators (IL-1β and TNF-α) and VEGF in MDA-MB-231 cells. qPCR showing the effect of Cx43 overexpression on IL-1β mRNA levels (A), TNF-α (B), VEGF (C). (D, E and F) Levels of secreted IL-1β, TNF-α and VEGF, respectively, as determined by ELISA. Results are representative of three different independent experiments. *, **, *** indicate $P < .05$, $P < .001$, $P < .0001$, respectively.

showed that Av treatment significantly increased IL-17, IL-6, IL-12a, IL-1β, TNF-α and RAGE and significantly decreased IL-10 mRNA levels, as compared to untreated cells (Fig. 1C and D).

Evaluation of secretion levels of TNF-α and IL-1β confirmed the data obtained by qPCR where their secretion levels increased by 75% following Av treatment (Fig. 1E).

Upregulation of pro-inflammatory cytokines mRNA and protein levels by Av treatment lead to the investigation of the NF-κB pathway activation and subsequent NF-κB translocation into the nucleus. Immunofluorescence revealed a significant increase in nuclear: cytoplasmic ratio of NF-κB in Av-treated cells (Fig. 2A and B). In addition, a significant increase in NF-κB p65 protein expression and IκB-α phosphorylation was observed accompanied by a significant decrease in IκB-α protein levels (Fig. 2C and D).

3.1.3. Av significantly down regulates transcriptional levels of VEGF while it significantly upregulates transcription of invasion and EMT markers

To examine the effect of Av on angiogenic, communication and EMT genes, we studied the expression of VEGF, Cx43, MMP2, MMP9, Twist, Snail, N-Cadherin and *E*-Cadherin (E-Cad) by qPCR. Av significantly downregulated VEGF mRNA expression (Fig. 3A) but showed no effect on Cx43 mRNA levels at 24 h of Av treatment (Fig. 3B and C). In addition, Av caused a time-dependent increase in Twist, Snail, N-Cadherin, MMP2 and MMP9 (Figs. 4 and 5A and B), and concurrently resulted in a time-dependent decrease in E-Cadherin mRNA levels, a mesenchymal-to-epithelial marker, reaching a maximal 50% decrease at 48 h following Av treatment (Fig. 4D).

3.1.4. Av treatment increases migration and invasion of MDA-MB-231 cells

The enzymatic activities of MMP2 and MMP9 showed a time-dependent increase, 24 h and 48 h after Av treatment of MDA-MB-231 cells as revealed by Gelatin zymography (Fig. 5C). This increase was correlated with a higher invasive potential of MDA-MB-231 cells following Av treatment (Fig. 5D).

3.1.5. Overexpression of Cx43 enhances the sensitivity of MDA-MB-231 cells to Av

We next investigated the effect of Cx43 overexpression on Av-induced inflammation. Overexpression of Cx43 in MDA-MB-231 cells lead to a significant decrease of the protein levels of NF-κB p65 and phosphorylated IκBα and to a decrease of the levels of transcripts of inflammatory mediators (IL-1β and TNF-α) and the angiogenic factor, VEGF. Consistently, Av treatment of MDA-Cx43D cells caused a similar decrease in NF-κB pathway components as compared to untreated cells (Figs. 6 and 7). Furthermore, Av-treated MDA-Cx43D cells showed a decrease in the protein expression levels of CD44, a target of NF-κB signaling. Fig. 6E, shows a shift of the histogram to the left indicative of a decrease in mean fluorescence intensity (MFI) and thus of CD44 protein expression levels in Av-treated cells. Immunofluorescence showed a significant decrease in nuclear: cytoplasmic ratio of NF-κB (Fig. 6C and D), further confirming that Cx43 overexpression alleviates the Av-induced inflammatory state in MDA-MB-231 cells. The decrease of NF-κB translocation in Av-treated MDA-Cx43D cells was paralleld by a decrease in the migration and invasion of Av-treated MDA-Cx43D cells (Fig. 8B and C), this was supported by a decreased MMP9 proteolytic activity (Fig. 8D and E).

3.2. In vivo study

3.2.1. Av treatment increases primary tumor volume and does not block metastasis in the xenograft mouse model

Av treatment increased the volume of primary tumors of NSG mice xenografted with MDA-MB-231 cells (Supplementary Fig. S1). Moreover, Av treatment failed to inhibit metastases of MDA-MB-231

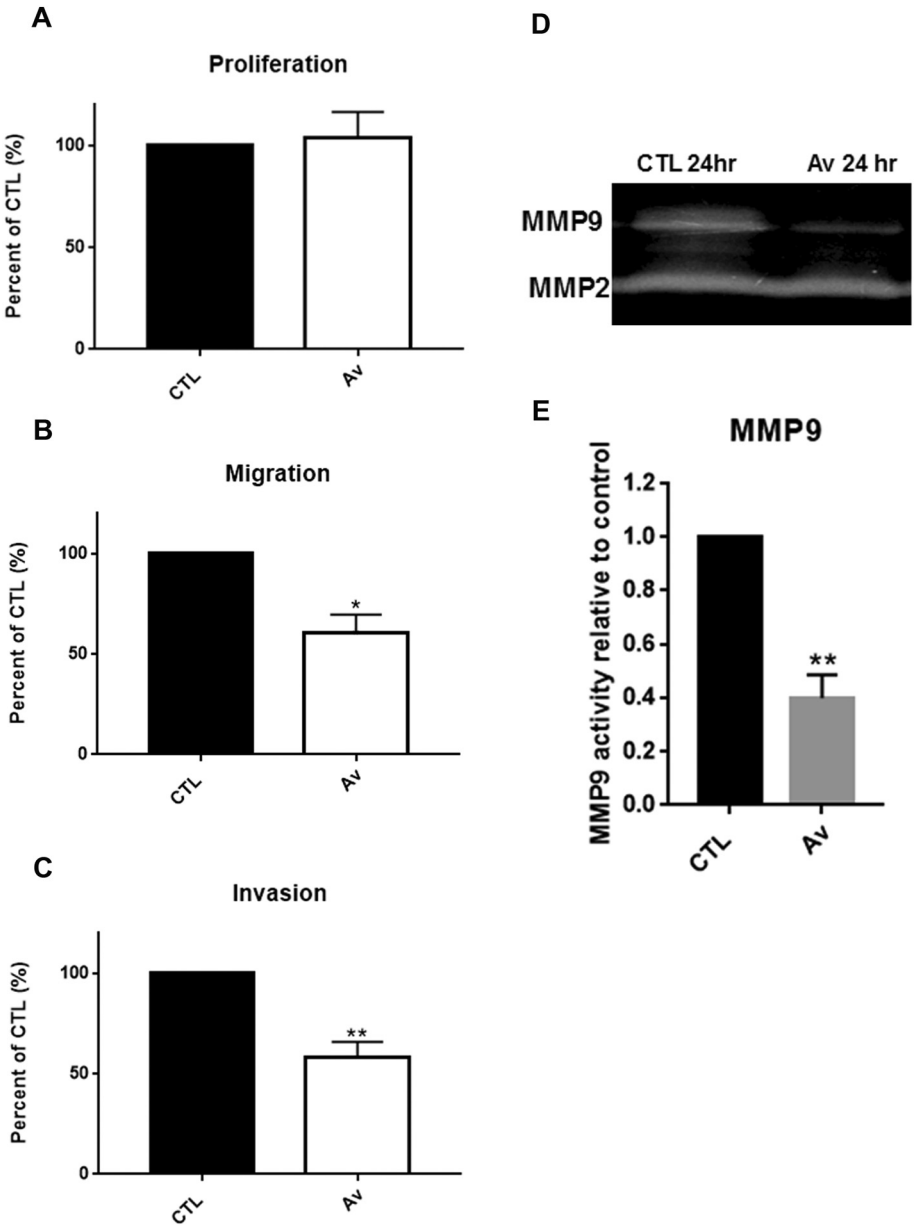

Fig. 8. Upregulation of Cx43 significantly decreases migration and invasion of MDA-Cx43D cells after Av treatment. (A) Proliferation, (B) Migration and (C) Invasion quantification graphs, as detected by Real-Time Cell Analysis (RTCA) assay, after normalizing cell index values to control untreated cells. Cell impedance readings were taken every 15 min for a minimum of 18 h. (D) Gelatin zymography of Av-treated MDA-Cx43D cells. FBS was used as an internal control. Proteins were separated on a gel containing gelatin, the substrate of MMPs, in order to assess the activation status and levels of these enzymes. (E) Quantification analysis MMP2 and MMP9 activity levels showing the effect of Cx43 overexpression on control and Av-treated cells. The intensity of each band was determined by densitometry, using Image Lab software. Quantification of each band was normalized to control. Results are representative of three different independent experiments. *, **, *** indicate $P < .05$, $P < .001$, $P < .0001$, respectively.

cells to the lungs of mice xenografted with MDA-MB-231 cells. Supplementary Fig. S2, shows that metastatic lesions have appeared in the lungs of both Av-treated or vehicle control xenografted mice.

3.2.2. Av treatment increases transcriptional expression of Cx43, N-Cadherin and inflammatory mediators

Next we assessed whether Av-induced inflammation in MDA-MB-231 cells in culture translates *in vivo* in the xenograft mouse model. mRNA levels of several of the markers acting during Av treatment of MDA-MB-231 *in vitro* were quantified by qPCR in metastatic lung tissues obtained from xenografted mice. Results showed a significant increase in the transcriptional level of IL-1β at week 5 which became more pronounced at week 9 following Av treatment. RAGE expression was also significantly increased at week 9 of Av treatment (Fig. 9A and B). Although VEGF and Cx43 expression significantly decreased at week 5, their expression increased at week 9 (Fig. 9A and B). Protein levels of NF-κB pathway components were also evaluated. At week 5 following xenograft, there was an increase in the protein levels of NF-κB pathway components including inflammatory mediators (TNF-α and IL-1β) as well as N-Cadherin (Fig. 9C and D). Immunofluorescence staining on lung tissues obtained from Av-treated xenografted mice further confirmed activation of inflammatory signaling pathways. Fig. 9G shows a significant increase in the phospohorylation of IκB-α. Surprisingly, at week 9 all inflammatory mediators showed a significant decrease (Fig. 9E and F). This was accompanied by a significant increase in Cx43 expression (Fig. 9E and F).

3.3. Archived cases of different breast cancer sub-types

3.3.1. Tumor tissues show higher expression of inflammatory mediators and a lower expression of anti-inflammatory cytokine (IL-10)

We assessed the inflammatory state in a cohort of breast carcinoma patients of different sub-types by measuring their mRNA levels using qPCR. Human breast tumor tissue showed a significant mRNA expression of RAGE, TNF-α and IL-1β but not IL-17 as compared to their non-cancerous counterparts (Fig. 10A, B, C and F). Whereas IL-13 expression was increased, IL-10 mRNA levels were significantly decreased (Fig. 10D and E). When comparing the three sub-types, we found that TNBC tissues showed significantly higher IL-17 mRNA levels accompanied by significantly lower levels of IL-13 as compared to normal

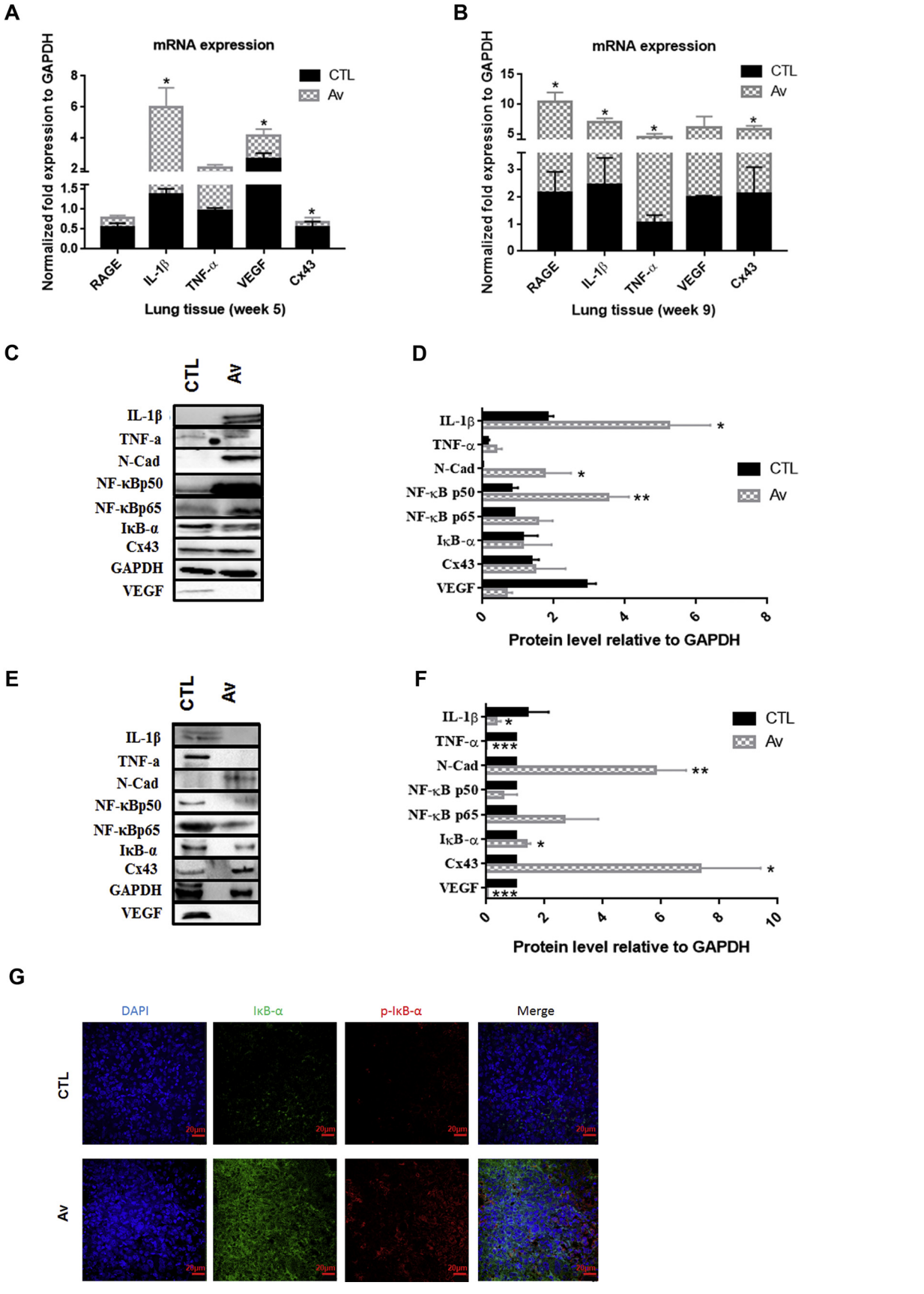

(caption on next page)

Fig. 9. Av affects the expression of inflammatory mediators, N-Cadherin and Cx43 in weeks 5 and 9 lung tissues of xenograft mice. (A) qPCR showing the effect of Av treatment in lung tissue at week 5 on IL-1β, TNF-α, VEGF, N-Cadherin, NF-κB p50, NF-κB p65, IκB-α and Cx43 mRNA expression, (B) at week 9. (C&D) Western blot and its quantification for IL-1β, TNF-α, VEGF, N-Cadherin, NF-κB p50, NF-κB p65, IκB-α, Cx43and GAPDH from lung tissue at week 5, (E&F) at week 9. Values represent the average fold change in IL-1β, TNF-α, VEGF, N-Cadherin, NF-κB p50, NF-κB p65, IκB-α and Cx43 expression, normalized to GAPDH, and relative to control lung tissue, for a total of three western blots. (G) Immunofluorescence staining of IκB-α and p-IκB-α in lung tissue at week 5. Results are representative of three different independent experiments. *, **, *** indicate $P < .05$, $P < .001$, $P < .0001$, respectively.

counter part breast tissue (Fig. 11). Interestingly, TNF-α mRNA levels were significantly lower levels in all groups of breast cancer patients (Fig. 11B).

4. Discussion

Tumor-promoting inflammation is an enabling characteristic of cancer [34]. Therapy-induced inflammation may lead to tumor re-emergence and resistance to treatment [35]. In this study we investigated whether cancer cells become refractory to Av due to therapy-induced inflammation using MDA-MB-231 human breast cancer cells *in vitro* and *in vivo*. We have shown that Av induced inflammation, where the NF-κB pathway and its down-stream components were activated. Data showed that Av treatment increased protein expression levels of NF-κB along with its translocation into the nucleus and decreased the protein levels of its regulatory protein, IκB [36]. After activation, NF-κB binds to promoter sequences of its target genes, which play key roles in cellular growth, inflammation and apoptosis [37]. Inflammatory mediators are prime NF-κB target genes, and in this study Av-activated NF-κB altered expression of several inflammatory mediators. Data on expression levels of RAGE, IL-1β and TNF-α, emphasizes this fact and illustrates the effect of Av on inflammation. In addition, constitutive activation of NF-κB has been also observed in breast [38], lung [39], lymphoma [40], and leukemia [41] cell lines. Moreover, increased NF-κB levels associate with poor prognostic consequences in glioblastoma [42] and ovarian cancer [43]. This can be explained by anti-tumor responses mediated by the inhibition of NF-κB signaling or by NF-κB gene knockout [44,45].

Av increased the expression of metalloproteinases (MMP2 and MMP9) and EMT markers (Twist and Snail). Consistent with our results, previous studies showed that NF-κB regulates expression of EMT markers [46]. Moreover, MMP2 and MMP9 are targets of many therapeutic treatments since their expression levels and activities are associated with higher invasive phenotypes [47]. Previous studies elucidated that downregulation of microRNA-138 enhances the proliferation, migration and invasion of cholangiocarcinoma cells through the upregulation of MMP2 and MMP9 [48].

Moreover, Av elicited an enhanced migration not only in metastatic cells such as MDA-MB-231 cells, but also in non-invasive MCF-7 cells (Fig. 2, in Data in Brief). Noteworthy, there was no change in the morphology of Av-treated MCF-7 cells, unlike Av-treated MDA-MB-231 which became more mesenchymal (Fig. 1, in Data in Brief).

MDA-MB-231 cells express low levels of Cx43 and have sparse intercellular communication. Surprisingly, upregulation of Cx43 alleviated the effect of Av on inflammation [27]. In fact, VEGF biosynthesis decreased upon upregulation of Cx43. This finding is in line with previous studies that reported the dominance of epithelial phenotype and attenuation of angiogenesis upon Cx43 upregulation [28]. Upregulation of Cx43 combined with Av treatment not only decreased the expression of inflammatory mediators but also decreased translocation of NF-κB. Moreover, it decreased the expression of CD44 that is involved in many cellular processes including cell adhesion and migration [49–52]. These observations are consistent with previous observations where inhibition of NF-κB lead to a decrease in CD44 expression which resulted in decreased cell proliferation and invasiveness of MDA-MB-231 cells [53]. In addition, our data showed that Av-treated MDA-MB-231 cells elicited a decrease in invasion and migration potential accompanied with a decrease in MMP9 activity. A previous study showed that, MMP9 down-regulation is associated with a decrease in invasion and vascularization of skin cancer [54].

In the *in vivo* assays, tumor cells were injected sub-dermally into the lower neck region where a primary tumor forms. This model allows the development of solid tumors at the site of injection, that later metastasize. Expression levels of inflammatory mediators were assessed in lung tissues harvested at weeks 5 and 9 following xenograft. Results confirmed the observations of *in vitro* studies. However, at week 9, the protein expression level of all mediators decreased while that of Cx43 significantly increased. This stated result matches with a previous work that reported that exposure to inflammatory conditions increases Cx43 expression [55]. Therefore, the observed decrease in inflammatory state at week 9 may be due to the induced upregulation of Cx43 which parallels the observation of *in vitro* study on cells upregulating Cx43.

Experiments done on human samples showed that inflammatory mediators (RAGE, TNF-α and IL-1β) are highly expressed in breast cancer specimens. Our finding comes in line with a previous study showing that TNF-α and IL-1β are highly expressed in tumor cells but not in normal breast epithelial cells [56]. Contrary to expectation, IL-17 showed low mRNA levels in tumor tissue. This may be explained by a study done by Muraski et al. showing that the adoptive transfer of Th_{17} cells results in pronounced regression and enhanced overall cure [57,58]. Therefore, for an untreated tumor tissue Th_{17} cells may be low especially in highly metastatic ones. This is also in accordance with the finding of Yang et al. who indicated that the count of T_{reg} but not Th_{17} cells is increased in breast cancer [59]. Together, these results suggest that expression of these potential mediators are confined either in the tissues adjacent to the breast tumor or in the tumor itself. This finding may have an effect on the systemic levels of these mediators and also on their biological effects at various stages of cancer progression in patients. Conversely, TNBC showed high levels of IL-17 and low levels of the anti-inflammatory cytokine IL-13. Given the lack of validated molecular targets and the poor outcome in patients with TNBC, it remains a chief challenge in today's clinical practice [60]. Our data highlight the fact that TNBC usually have high levels of inflammatory mediators, and the Av treatment further induces this inflammatory microenvironment. As a result, Av may increase the challenges of treating this type of cancer. Our findings come in accordance with previous work that identified only 32% of TNBC patients having low pro-inflammatory interleukin 8 had good prognosis [61].

Our study postulates that anti-angiogenesis therapy is more significant in tumors that express Cx43.

Supplementary data to this article can be found online at https://doi.org/10.1016/j.cellsig.2018.11.007.

Acknowledgements

Authors would like to thank Dr. Rémi Safi for her technical support and Dr. Najla Fakhruddin for providing the paraffin blocks of breast carcinoma tissues. This work was supported by grants from Lebanese National Council for Scientific Research, and from the Medical Practice Plan and University Research Board grants at the American University of Beirut (MES).

Author contributions

Conceived and designed the experiments: MES. Performed the experiments: LEH NJ JK. Analyzed the data: LEH NJ AS MES. Contributed

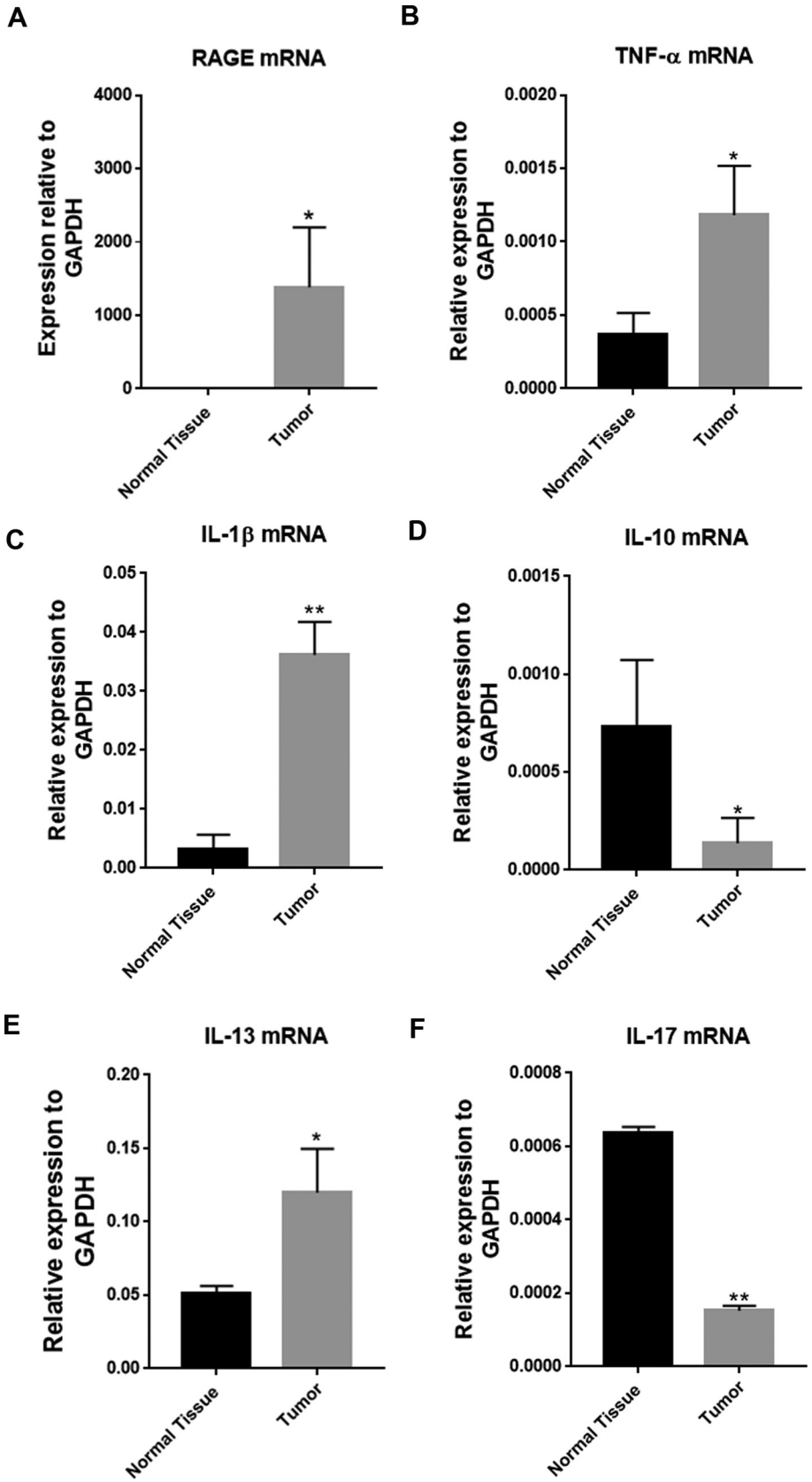

Fig. 10. Tumor tissues show increased expression of inflammatory mediator and decreased expression of anti-inflammatory cytokine (IL-10). qPCR showing mRNA expression of RAGE (A), TNF-α (B), IL-1β (C), IL-10 (D), IL-13 (E) and IL-17 (F). Data for each target mRNA were normalized to GAPDH. Results are representative of three different independent experiments. *, **, *** indicate $P < .05$, $P < .001$, $P < .0001$, respectively.

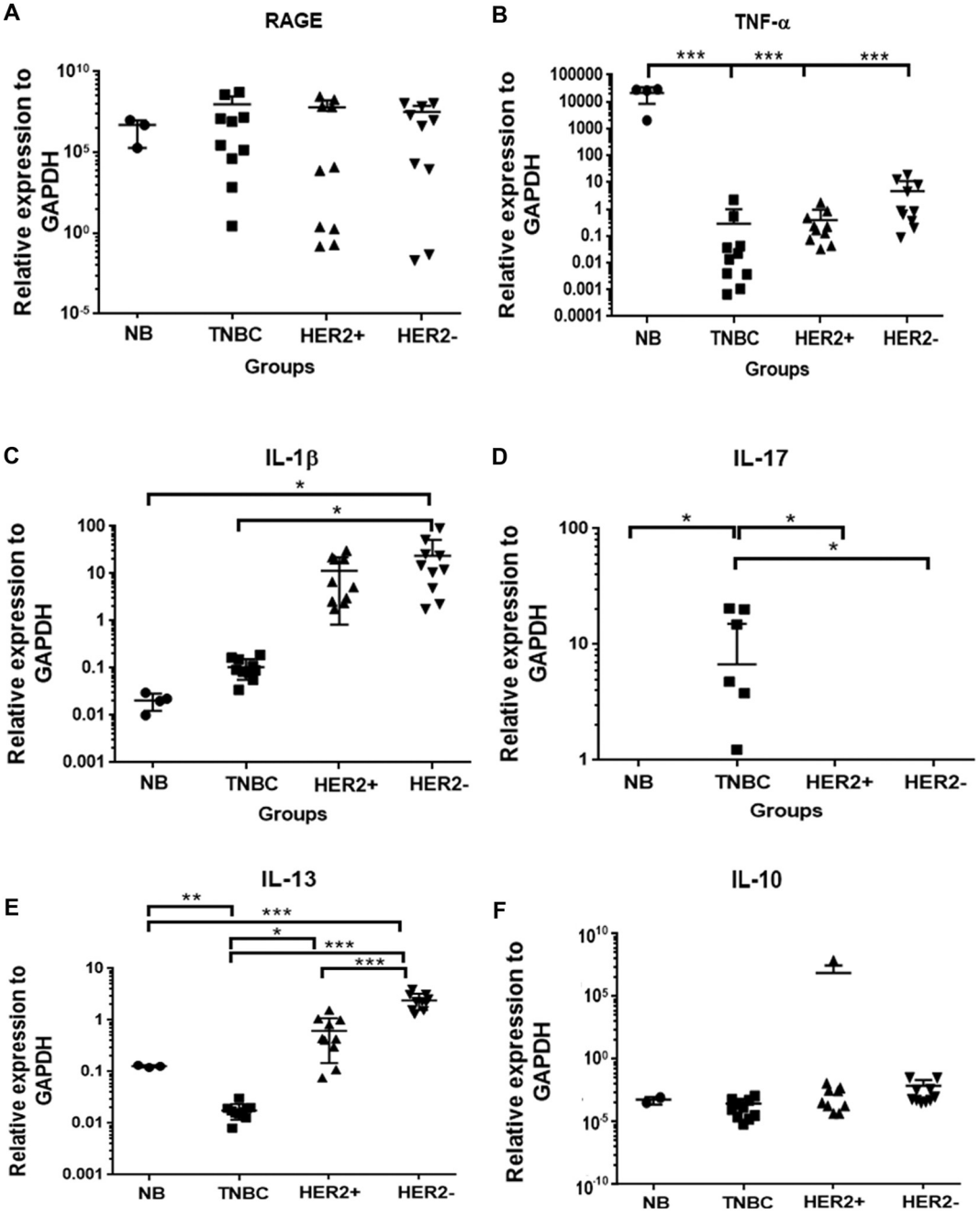

Fig. 11. TNBC show a low expression of inflammatory mediators when compared normal breast(NB)and to HER2+/HER2- breast tissues (Group 2&3 respectively). qTime PCR showing mRNA expression of RAGE (A),TNF-α (B), IL-1β (C), IL-17 (D), IL-13 (E) and IL-10 (F). Data for each target mRNA were normalized to GAPDH. Results are representative of 11 different patient specimen. *, **, *** indicate $P < .05$, $P < .001$, $P < .0001$, respectively.

reagents/materials/analysis tools: KZ JK. The manuscript was written by: LEH, critically reviewed by: AS JS and approved by MES.

Conflicts of interest

The authors declare no competing financial interests.

References

[1] R. Dent, M. Trudeau, K.I. Pritchard, W.M. Hanna, H.K. Kahn, C.A. Sawka, L.A. Lickley, E. Rawlinson, P. Sun, S.A. Narod, Triple-negative breast cancer: clinical features and patterns of recurrence, Clin. Cancer Res. 13 (2007) 4429–4434.

[2] B.G. Haffty, Q. Yang, M. Reiss, T. Kearney, S.A. Higgins, J. Weidhaas, L. Harris, W. Hait, D. Toppmeyer, Locoregional relapse and distant metastasis in conservatively managed triple negative early-stage breast cancer, J. Clin. Oncol. 24 (2006) 5652–5657.

[3] J. Reis-Filho, A. Tutt, Triple negative tumours: a critical review, Histopathology 52 (2008) 108–118.

[4] K.R. Bauer, M. Brown, R.D. Cress, C.A. Parise, V. Caggiano, Descriptive analysis of estrogen receptor (ER)-negative, progesterone receptor (PR)-negative, and HER2-negative invasive breast cancer, the so-called triple-negative phenotype, Cancer 109 (2007) 1721–1728.

[5] M. Tischkowitz, J.-S. Brunet, L.R. Bégin, D.G. Huntsman, M.C. Cheang, L.A. Akslen, T.O. Nielsen, W.D. Foulkes, Use of immunohistochemical markers can refine prognosis in triple negative breast cancer, BMC Cancer 7 (2007) 134.

[6] A. Ishihara, H. Tsuda, K. Kitagawa, M. Yoneda, T. Shiraishi, Morphological characteristics of basal-like subtype of breast carcinoma with special reference to cytopathological features, Breast Cancer 16 (2009) 179–185.

[7] L. Fulford, D. Easton, J. Reis-Filho, A. Sofronis, C. Gillett, S. Lakhani, A. Hanby, Specific morphological features predictive for the basal phenotype in grade 3 invasive ductal carcinoma of breast, Histopathology 49 (2006) 22–34.

[8] H.-P. Gerber, T.H. Vu, A.M. Ryan, J. Kowalski, Z. Werb, N. Ferrara, VEGF couples hypertrophic cartilage remodeling, ossification and angiogenesis during

endochondral bone formation, Nat. Med. 5 (1999) 623–628.
[9] A. Saaristo, T. Karpanen, K. Alitalo, Mechanisms of angiogenesis and their use in the inhibition of tumor growth and metastasis, Oncogene 19 (2000).
[10] G. Bergers, D. Hanahan, Modes of resistance to anti-angiogenic therapy, Nat. Rev. Cancer 8 (2008) 592–603.
[11] M. Delay, A. Jahangiri, W.S. Carbonell, Y.-L. Hu, S. Tsao, M.W. Tom, J. Paquette, T.A. Tokuyasu, M.K. Aghi, Microarray analysis verifies two distinct phenotypes of glioblastomas resistant to antiangiogenic therapy, Clin. Cancer Res. 18 (2012) 2930–2942.
[12] K.V. Lu, G. Bergers, Mechanisms of Evasive Resistance to Anti-VEGF Therapy in Glioblastoma, (2012).
[13] N.N. Rahbari, D. Kedrin, J. Incio, H. Liu, W.W. Ho, H.T. Nia, C.M. Edrich, K. Jung, J. Daubriac, I. Chen, Anti-VEGF therapy induces ECM remodeling and mechanical barriers to therapy in colorectal cancer liver metastases, Sci. Transl. Med. 8 (2016) 360ra135.
[14] J. Waltenberger, VEGF Resistance as a Molecular Basis to Explain the Angiogenesis Paradox in Diabetes Mellitus, Portland Press Limited, 2009.
[15] J. Rius, M. Guma, C. Schachtrup, K. Akassoglou, A.S. Zinkernagel, V. Nizet, R.S. Johnson, G.G. Haddad, M. Karin, NF-κB links innate immunity to the hypoxic response through transcriptional regulation of HIF-1α, Nature 453 (2008) 807.
[16] A. Carbia-Nagashima, J. Gerez, C. Perez-Castro, M. Paez-Pereda, S. Silberstein, G.K. Stalla, F. Holsboer, E. Arzt, RSUME, a small RWD-containing protein, enhances SUMO conjugation and stabilizes HIF-1α during hypoxia, Cell 131 (2007) 309–323.
[17] C.T. Taylor, Interdependent roles for hypoxia inducible factor and nuclear factor-κB in hypoxic inflammation, J. Physiol. 586 (2008) 4055–4059.
[18] K. Gutsche, E.B. Randi, V. Blank, D. Fink, R.H. Wenger, C. Leo, C.C. Scholz, Intermittent hypoxia confers pro-metastatic gene expression selectively through NF-κB in inflammatory breast cancer cells, Free Radic. Biol. Med. 101 (2016) 129–142.
[19] T. Leibovich-Rivkin, Y. Liubomirski, B. Bernstein, T. Meshel, A. Ben-Baruch, Inflammatory factors of the tumor microenvironment induce plasticity in non-transformed breast epithelial cells: EMT, invasion, and collapse of normally organized breast textures, Neoplasia 15 (2013) 1330IN1334–1346IN1335.
[20] M.E. El-Sabban, R.A. Merhi, H.A. Haidar, B. Arnulf, H. Khoury, J. Basbous, J. Nijmeh, O. Hermine, A. Bazarbachi, Human T-cell lymphotropic virus type 1–transformed cells induce angiogenesis and establish functional gap junctions with endothelial cells, Blood 99 (2002) 3383–3389.
[21] A. Bazarbachi, R.A. Merhi, A. Gessain, R. Talhouk, H. El-Khoury, R. Nasr, O. Gout, R. Sulahian, F. Homaidan, O. Hermine, Human T-cell lymphotropic virus type I-infected cells extravasate through the endothelial barrier by a local angiogenesis-like mechanism, Cancer Res. 64 (2004) 2039–2046.
[22] Y. Kanno, W.R. Loewenstein, Low-resistance coupling between gland cells. Some observations on intercellular contact membranes and intercellular space, Nature 201 (1964) 194–195.
[23] C.-J. Wei, X. Xu, C.W. Lo, Connexins and cell signaling in development and disease, Annu. Rev. Cell Dev. Biol. 20 (2004) 811–838.
[24] D.B. Alexander, G.S. Goldberg, Transfer of biologically important molecules between cells through gap junction channels, Curr. Med. Chem. 10 (2003) 2045–2058.
[25] R.C. Pimentel, K.A. Yamada, A.G. Kléber, J.E. Saffitz, Autocrine regulation of myocyte Cx43 expression by VEGF, Circ. Res. 90 (2002) 671–677.
[26] X. Wu, W. Huang, G. Luo, L.A. Alain, Hypoxia induces connexin 43 dysregulation by modulating matrix metalloproteinases via MAPK signaling, Mol. Cell. Biochem. 384 (2013) 155–162.
[27] H. Qin, Q. Shao, H. Curtis, J. Galipeau, D.J. Belliveau, T. Wang, M.A. Alaoui-Jamali, D.W. Laird, Retroviral delivery of connexin genes to human breast tumor cells inhibits in vivo tumor growth by a mechanism that is independent of significant gap junctional intercellular communication, J. Biol. Chem. 277 (2002) 29132–29138.
[28] E. McLachlan, Q. Shao, H.-l. Wang, S. Langlois, D.W. Laird, Connexins act as tumor suppressors in three-dimensional mammary cell organoids by regulating differentiation and angiogenesis, Cancer Res. 66 (2006) 9886–9894.
[29] W.-K. Wang, M.-C. Chen, H.-F. Leong, Y.-L. Kuo, C.-Y. Kuo, C.-H. Lee, Connexin 43 suppresses tumor angiogenesis by down-regulation of vascular endothelial growth factor via hypoxic-induced factor-1α, Int. J. Mol. Sci. 16 (2014) 439–451.
[30] S. Al-Ghadban, S. Kaissi, F.R. Homaidan, H.Y. Naim, M.E. El-Sabban, Cross-talk between intestinal epithelial cells and immune cells in inflammatory bowel disease, Sci. Rep. 6 (2016) 29783.
[31] D.R. Emlet, K.A. Brown, D.L. Kociban, A.A. Pollice, C.A. Smith, B.B.L. Ong, S.E. Shackney, Response to trastuzumab, erlotinib, and bevacizumab, alone and in combination, is correlated with the level of human epidermal growth factor receptor-2 expression in human breast cancer cell lines, Mol. Cancer Ther. 6 (2007) 2664–2674.
[32] K. Zibara, Z. Awada, L. Dib, J. El-Saghir, S. Al-Ghadban, A. Ibrik, N. El-Zein, M. El-Sabban, Anti-angiogenesis therapy and gap junction inhibition reduce MDA-MB-231 breast cancer cell invasion and metastasis in vitro and in vivo, Sci. Rep. 5 (2015) 12598.
[33] Z. Teng, X. Kuang, J. Wang, X. Zhang, Real-time cell analysis–a new method for dynamic, quantitative measurement of infectious viruses and antiserum neutralizing activity, J. Virol. Methods 193 (2013) 364–370.
[34] D. Hanahan, R.A. Weinberg, Hallmarks of cancer: the next generation, Cell 144 (2011) 646–674.
[35] S.I. Grivennikov, F.R. Greten, M. Karin, Immunity, inflammation, and cancer, Cell 140 (2010) 883–899.
[36] S. Ghosh, M.J. May, E.B. Kopp, NF-κB and Rel proteins: evolutionarily conserved mediators of immune responses, Annu. Rev. Immunol. 16 (1998) 225–260.
[37] H.L. Pahl, Activators and target genes of Rel/NF-κB transcription factors, Oncogene 18 (1999).
[38] H. Chua, P. Bhat-Nakshatri, S. Clare, A. Morimiya, S. Badve, H. Nakshatri, NF-κB represses E-cadherin expression and enhances epithelial to mesenchymal transition of mammary epithelial cells: potential involvement of ZEB-1 and ZEB-2, Oncogene 26 (2007) 711–724.
[39] G.W. Tew, E.L. Lorimer, T.J. Berg, H. Zhi, R. Li, C.L. Williams, SmgGDS regulates cell proliferation, migration, and NF-κB transcriptional activity in non-small cell lung carcinoma, J. Biol. Chem. 283 (2008) 963–976.
[40] P. Zou, J. Kawada, L. Pesnicak, J.I. Cohen, Bortezomib induces apoptosis of Epstein-Barr virus (EBV)-transformed B cells and prolongs survival of mice inoculated with EBV-transformed B cells, J. Virol. 81 (2007) 10029–10036.
[41] T. Vilimas, J. Mascarenhas, T. Palomero, M. Mandal, S. Buonamici, F. Meng, B. Thompson, C. Spaulding, S. Macaroun, M.-L. Alegre, Targeting the NF-κB signaling pathway in Notch1-induced T-cell leukemia, Nat. Med. 13 (2007) 70–77.
[42] R.E. Brown, A. Law, Morphoproteomic demonstration of constitutive nuclear factor-kappaB activation in glioblastoma multiforme with genomic correlates and therapeutic implications, Ann. Clin. Lab. Sci. 36 (2006) 421–426.
[43] C.M. Annunziata, H.T. Stavnes, L. Kleinberg, A. Berner, L.F. Hernandez, M.J. Birrer, S.M. Steinberg, B. Davidson, E.C. Kohn, Nuclear factor κB transcription factors are coexpressed and convey a poor outcome in ovarian cancer, Cancer 116 (2010) 3276–3284.
[44] Y. Li, F. Ahmed, S. Ali, P.A. Philip, O. Kucuk, F.H. Sarkar, Inactivation of nuclear factor κB by soy isoflavone genistein contributes to increased apoptosis induced by chemotherapeutic agents in human cancer cells, Cancer Res. 65 (2005) 6934–6942.
[45] E. Meylan, A.L. Dooley, D.M. Feldser, L. Shen, E. Turk, C. Ouyang, T. Jacks, Requirement for NF-&kgr; B signalling in a mouse model of lung adenocarcinoma, Nature 462 (2009) 104–107.
[46] Y. Kim, H. Park, D. Jeoung, CAGE, a cancer/testis antigen, induces c-FLIPL and Snail to enhance cell motility and increase resistance to an anti-cancer drug, Biotechnol. Lett. 31 (2009) 945–952.
[47] A. Laios, B.M. Mohamed, L. Kelly, R. Flavin, S. Finn, L. McEvoy, M. Gallagher, C. Martin, O. Sheils, M. Ring, Pre-treatment of platinum resistant ovarian cancer cells with an MMP-9/MMP-2 inhibitor prior to cisplatin enhances cytotoxicity as determined by high content screening, Int. J. Mol. Sci. 14 (2013) 2085–2103.
[48] Q. Wang, H. Tang, S. Yin, C. Dong, Downregulation of microRNA-138 enhances the proliferation, migration and invasion of cholangiocarcinoma cells through the up-regulation of RhoC/p-ERK/MMP-2/MMP-9, Oncol. Rep. 29 (2013) 2046–2052.
[49] H. Ponta, L. Sherman, P.A. Herrlich, CD44: from adhesion molecules to signalling regulators, Nat. Rev. Mol. Cell Biol. 4 (2003) 33–45.
[50] M. Zöller, CD44: can a cancer-initiating cell profit from an abundantly expressed molecule? Nat. Rev. Cancer 11 (2011) 254–267.
[51] L. Hebbard, A. Steffen, V. Zawadzki, C. Fieber, N. Howells, J. Moll, H. Ponta, M. Hofmann, J. Sleeman, CD44 expression and regulation during mammary gland development and function, J. Cell Sci. 113 (2000) 2619–2630.
[52] P. Herrlich, H. Morrison, J. Sleeman, V. Orian-Rousseau, H. König, S. Weg-Remers, H. Ponta, CD44 acts both as a growth-and invasiveness-promoting molecule and as a tumor-suppressing cofactor, Ann. N. Y. Acad. Sci., 910 (2000) 106–120.
[53] S.M. Smith, Y.L. Lyu, L. Cai, NF-κB affects proliferation and invasiveness of breast cancer cells by regulating CD44 expression, PLoS One 9 (2014) e106966.
[54] E.C. Woenne, W. Lederle, S. Zwick, M. Palmowski, H. Krell, W. Semmler, M.M. Mueller, F. Kiessling, MMP inhibition blocks fibroblast-dependent skin cancer invasion, reduces vascularization and alters VEGF-A and PDGF-BB expression, Anticancer Res. 30 (2010) 703–711.
[55] B.C. Avendaño, T.D. Montero, C.E. Chávez, R. von Bernhardi, J.A. Orellana, Prenatal exposure to inflammatory conditions increases Cx43 and Panx1 unopposed channel opening and activation of astrocytes in the offspring effect on neuronal survival, Glia 63 (2015) 2058–2072.
[56] G. Soria, M. Ofri-Shahak, I. Haas, N. Yaal-Hahoshen, L. Leider-Trejo, T. Leibovich-Rivkin, P. Weitzenfeld, T. Meshel, E. Shabtai, M. Gutman, Inflammatory mediators in breast cancer: coordinated expression of TNFα & IL-1β with CCL2 & CCL5 and effects on epithelial-to-mesenchymal transition, BMC Cancer 11 (2011) 130.
[57] I. Kryczek, M. Banerjee, P. Cheng, L. Vatan, W. Szeliga, S. Wei, E. Huang, E. Finlayson, D. Simeone, T.H. Welling, Phenotype, distribution, generation, and functional and clinical relevance of Th17 cells in the human tumor environments, Blood 114 (2009) 1141–1149.
[58] P. Muranski, A. Boni, P.A. Antony, L. Cassard, K.R. Irvine, A. Kaiser, C.M. Paulos, D.C. Palmer, C.E. Touloukian, K. Ptak, Tumor-specific Th17-polarized cells eradicate large established melanoma, Blood 112 (2008) 362–373.
[59] L. Yang, Y. Qi, J. Hu, L. Tang, S. Zhao, B. Shan, Expression of Th17 cells in breast cancer tissue and its association with clinical parameters, Cell Biochem. Biophys. 62 (2012) 153–159.
[60] K.J. Chavez, S.V. Garimella, S. Lipkowitz, Triple negative breast cancer cell lines: one tool in the search for better treatment of triple negative breast cancer, Breast Dis. 32 (2010) 35.
[61] A. Rody, T. Karn, C. Liedtke, L. Pusztai, E. Ruckhaeberle, L. Hanker, R. Gaetje, C. Solbach, A. Ahr, D. Metzler, A clinically relevant gene signature in triple negative and basal-like breast cancer, Breast Cancer Res. 13 (2011) R97.